

## Nonequilibrium Roughening and Faceting of Interfaces in Driven Alloys

P. Bellon

*Department of Materials Science and Engineering, 1304 W. Green Street, Urbana, Illinois 61801*

(Received 28 January 1998)

We consider the case of crystalline alloys submitted to an external forcing that produces ballistic atom exchanges. The dynamical stability of precipitate-matrix interfaces is studied by kinetic atomistic Monte Carlo simulations. At steady state, sharp precipitate-matrix interfaces can exhibit kinetic roughening, while diffuse interfaces may develop a surprising kinetic faceting. The latter results in nonequilibrium faceted shapes for precipitates. The possible implications for materials subjected to radiation fields or processed by ion beams are discussed. [S0031-9007(98)07663-7]

PACS numbers: 61.80.-x, 05.70.Ln, 68.35.Ct

Materials in service or during their elaboration are often submitted to some sustained external forcing that drives them out of equilibrium (for a review, see [1]). Such is the case during vapor phase growth because of the impingement of atoms onto the growth surface; or during irradiation because of the replacements and displacements of atoms produced by nuclear collisions, or during plastic deformation because of dislocation glide. The composition field, the chemical order field, or the microstructure of these driven solids may eventually reach a steady state. By varying the forcing conditions, dynamical transitions are observed to take place between various steady states. For instance, immiscible elements can be stabilized into a solid solution by low temperature irradiation [2] or ball milling [3], while enhanced decomposition takes place when the temperature is raised. The nature and stability of these steady states are important since they may alter the alloy properties.

A generic approach to model and study driven alloys is based on kinetic models where a forced dynamics produced by the external forcing is competing with a thermally activated dynamics [1,4-7]. In such systems, interfaces display a wide range of behaviors [8]; e.g., when the forced dynamics results from an applied electrical field, interfacial roughness can be suppressed, due to the anisotropy of that forced dynamics [9]. However, in crystals under shearing, the glide of dislocations creates large perturbations at coherent interfaces, and this results in a large power-law roughening [10]. This kinetic roughening leads to the stabilization of new stable structures that are decomposed at a mesoscopic scale. The general properties of interfaces in driven alloys remain largely to be explored, as well as the potential consequences for microstructural evolutions.

We consider here a crystalline alloy where atoms can migrate through thermally activated exchanges at a finite temperature  $T$  with vacancies. This alloy is also exposed to an external forcing that produces ballistic exchanges between nearest-neighbor atoms at a controlled frequency,  $\Gamma_b$ . It has been introduced by Martin to model alloys under irradiation [11]. Using Monte Carlo simulations,

we show that by varying the control parameters,  $T$  and  $\Gamma_b$ , the external forcing may lead either to the kinetic roughening of interfaces or, more surprisingly, to their kinetic faceting.

For the Monte Carlo simulations, a face-centered cubic (fcc) crystal is constructed from a  $N_1 \times N_1 \times N_2$  ( $N_{1,2} = 16$  to  $256$ ) simple rhombohedral crystal with periodic boundary conditions (unless stated otherwise). The faces of the rhombohedron correspond to  $\{111\}$  planes of the fcc crystal. A binary  $A_x B_{1-x}$  model alloy is considered, with a moderate positive heat of mixing, typical of the Cu-Co system. The critical temperature of the miscibility gap,  $T_c$ , is therefore set to 1573 K, by choosing an appropriate negative first nearest-neighbor ordering energy (atom interactions are here restricted to pairwise energies between nearest-neighbor atoms,  $\epsilon_{ij}$  with  $i, j = A, B$ ). Thermally activated diffusion takes place due to the migration of a vacancy: The vacancy migration energy is set to 0.8 eV in pure  $A$  or pure  $B$ , and the attempt frequency is set to give a preexponential diffusion coefficient of  $10^{-5} \text{ m}^2 \text{ s}^{-1}$ , values that are typical for copper (see Ref. [10] for more details). Whatever the size of the crystal, only one vacancy is introduced in the crystal to avoid complications arising from the formation of vacancy clusters. When the system size is varied the vacancy concentration,  $c_v$ , changes, and so we rescale the ballistic jump frequency  $\Gamma_b$  accordingly, to get meaningful comparisons. All  $\Gamma_b$  numerical values reported here are for  $c_v = 1/64^3$ .

A residence-time algorithm is used to construct a kinetic evolution of the system, through vacancy jumps and ballistic exchanges, and to calculate the time spent by the system in each microscopic configuration [1]. As a result of ballistic jumps, atomic solubilities are increased, and to define interfaces a coarse graining procedure is required to eliminate bulk composition fluctuations [12]. The initial rhombohedron lattice of parameter  $a$  is coarse grained into a simple cubic lattice of parameter  $\sqrt{2}a$  following a one-step coarse graining detailed elsewhere [10].

We first study the stability of bilayer configurations. Crystals containing one  $A/B$  bilayer with flat  $\{111\}$  or  $\{100\}$  interfaces are created by using periodic and

helicoidal boundary conditions, respectively. In both cases, the interfacial area is proportional to  $N_1^2$  and the thickness of the bilayer is proportional to  $N_2$ . These two orientations correspond to the smallest values for the interfacial excess internal energy [13]. To characterize these interfaces, after coarse graining, the height of an interface  $h(\mathbf{r})$ , at point  $\mathbf{r}$ , and the average height of the interface  $\langle h \rangle$  are calculated, as well as the circularly averaged height-to-height correlation function,  $G(r) = \langle H(\mathbf{0})H(\mathbf{r}) \rangle_C$ , where  $H(\mathbf{r}) = h(\mathbf{r}) - \langle h \rangle$ . This gives the width of the interface as  $\sigma = G(0)^{1/2}$ .

Figure 1 shows the evolution of the steady-state width for  $\{111\}$  and  $\{100\}$  interfaces,  $\sigma_{\{111\}}$  and  $\sigma_{\{100\}}$ , as a function of  $\Gamma_b$  while keeping the temperature fixed. Both interfaces undergo a discontinuous transition from a faceted shape to a rough shape. The discontinuity is large for the  $\{111\}$  orientation and is associated with a hysteresis loop for  $0.14 < \Gamma_b < 0.45$  when the total number of jumps in one run is set to  $5 \times 10^{10}$ . In this interval, the system is bistable and the selection of the final steady state (upper or lower branch of the hysteresis loop) is determined by the initial configuration. These results indicate that these dynamical transitions are of first order. Notice that, at large enough  $\Gamma_b$  values, the width of  $\{100\}$  interfaces decreases with  $\Gamma_b$ .

Beyond these transitions ( $\Gamma_b \geq 0.5 \text{ s}^{-1}$ ), the unique steady-state value for  $\sigma$  is studied as a function of  $N_1$ : first, in the regime where  $\sigma_{\{111\}}$  and  $\sigma_{\{100\}}$  increase with  $\Gamma_b$ , second, in the regime where  $\sigma_{\{100\}}$  decreases with  $\Gamma_b$ . In the first regime, the increase of  $\sigma_{\{100\}}$  (Fig. 2) and  $\sigma_{\{111\}}$  (not shown) with  $N_1$  establishes the presence of kinetic roughening. For both interfaces, a power-law fit indicates that the local exponent tends to decrease with  $N_1$ , probably because of finite-size effects at small  $N_1$

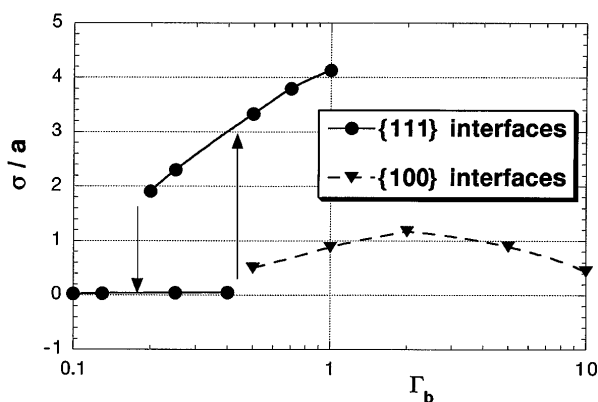


FIG. 1. Steady-state width of interfaces as a function of the ballistic jump frequency at  $T = 400 \text{ K}$ . Note the large hysteresis loop for  $\{111\}$  orientations. No data could be recorded for this orientation beyond  $\Gamma_b = 1 \text{ s}^{-1}$  since the interface forms  $\{100\}$  facets. For the sake of clarity, no data is shown for  $\{100\}$  orientations at low  $\Gamma_b$  values. Data are averages obtained over more than 100 independent measurements. The simulation cell is  $64^3$ .

values. For  $N_1 > 64$ ,  $\alpha = 1.15$  is measured for  $\{100\}$  interfaces. As discussed below, an asymptotic value  $\alpha = 1$  is in fact expected. In the second regime, a surprising kinetic faceting of  $\{100\}$  interfaces is observed:  $\sigma_{\{100\}}$  takes a low value independent of  $N_1$  (Fig. 2).

The kinetic roughening observed in Fig. 2 is accompanied by the formation of mounds, and steady state is obtained after the coarsening of these mounds, leading to the presence one single large mound in the simulation cell. Similar mound formation has been reported in the case of growth surfaces at moderate temperatures. In the latter case, mound instability occurs when atomic steps introduce a bias for adatom diffusion, bias that either suppresses adatom migration across descending steps [14] (due to positive Ehrlich-Schwoebel barriers) or favors adatom migration towards ascending steps [15]. Here we are concerned with the vacancy-assisted migration of pseudoatoms on flat interfaces and across interfacial steps. We have calculated the activation barriers involved in this migration, and, similar to the case of surfaces, we have found diffusion biases when a pseudoatom approaches an interfacial step (a detailed study will be presented elsewhere).

The origin of these diffusion biases in our diffusion model differs somewhat from those found at surfaces: To reach a step, a pseudoatom needs to exchange with a vacancy located at the step edge; it is the jumps that allow a vacancy to reach such a step edge that have their activation barrier modified by the presence of the step edge. Indeed, some atoms have more homoatomic bonds there than on a flat terrace; these atoms are thus more strongly bound, and activation barriers to exchange these atoms with a vacancy are increased. For instance, this results in vacancy jump frequencies that are enhanced (respectively, lowered) by a factor  $\exp\{2(\epsilon_{AB} - \epsilon_{BB})/kT\}$  [respectively,  $\exp\{(\epsilon_{AB} - \epsilon_{BB})/kT\}$ ] at an ascending (respectively, descending) step in the case of a  $B$  pseudoatom

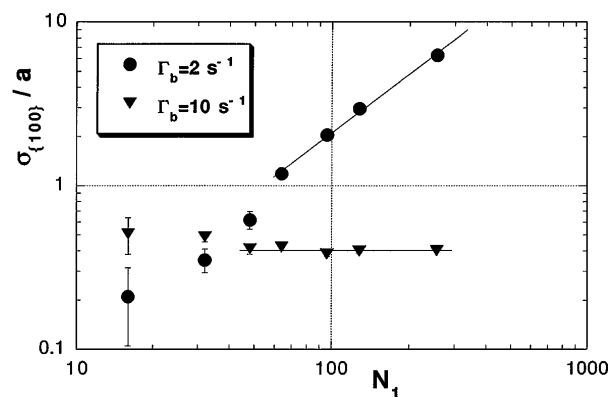


FIG. 2. Steady-state width of interfaces as a function of  $N_1$  for  $\{100\}$  orientations at  $\Gamma_b = 2 \text{ s}^{-1}$  (kinetic roughening) and at  $\Gamma_b = 10 \text{ s}^{-1}$  (kinetic faceting). Data are obtained at  $T = 400 \text{ K}$  and for  $N_2 = 64$ . Solid lines are guides for the eye. Error bars represent one standard deviation.

approaching a  $[011]$  step on a  $\{100\}$  interface. For the present setting, these factors are 4.96 and 2.23, respectively, and are thus large enough to destabilize initially flat interfaces [16]. The simplicity and the generality of this phenomenon indicate that adatom diffusion biases should exist at coherent interfaces in general, beyond the limitations of the present atomic diffusion model.

The destabilizing effect of these diffusion biases is competing with the interfacial smoothing promoted by bulk diffusion (analog to evaporation-condensation in the case of surfaces). Simple continuum models [14,17] with these two competing effects predict the formation of rough interfaces that exhibit slope selection. This corresponds to a roughening exponent  $\alpha = 1$ , in good agreement with our results for large system sizes (Fig. 2).

The kinetic faceting observed in Fig. 2 is quite remarkable. It seems counterintuitive since the larger the  $\Gamma_b$ , the more “disordered” the interface should be. A crucial element used to understand this kinetic faceting is that  $\{100\}$  interfaces have become slightly diffuse (typically, over four atomic layers) as a result of more frequent ballistic jumps. The diffuseness of these interfaces prevents the instability mechanism described above to operate, and the interface, on a scale larger than its diffuseness, remains flat. Indeed, kinetic faceting is only observed for  $(T, \Gamma_b)$  values that result in diffuse interfaces. The  $\{111\}$  interfaces do not exhibit kinetic faceting: They are sharp and thus rough at moderately high  $\Gamma_b$  values, and increasing  $\Gamma_b$  results in an increase of the roughness and in the local formation of  $\{100\}$  facets. Ballistic mixing is expected to be less efficient for  $\{111\}$  interfaces since one-half of nearest-neighbor bonds lie out of plane, compared to two-third for  $\{100\}$  interfaces. By extension, it is predicted that refaceting will take place for orientations having a large fraction of nearest neighbors out of plane, i.e., for orientations where the excess interfacial energy is large. This kinetic faceting should thus stabilize nonequilibrium interface orientations.

This kinetic roughening and faceting of interfaces suggests that precipitates may exhibit dynamical shape transitions. Figure 3 displays the typical precipitate shapes reached at steady state at temperature  $T = 400$  K for  $N_1 = N_2 = 64$  crystals. At  $\Gamma_b = 0$  [Fig. 3(a)], the steady-state shape is the equilibrium shape of the precipitate, and, as expected at this temperature for an alloy on an fcc lattice with only nearest-neighbor interactions, the shape mostly consists of  $\{111\}$  facets, with some smaller  $\{100\}$  facets [13]. At nonzero but rather moderate ballistic frequency,  $\Gamma_b = 0.5 \text{ s}^{-1}$  in Fig. 3(b), the steady-state shape of the precipitate is close to that of a sphere, with some small  $\{111\}$ ,  $\{100\}$ , and  $\{110\}$  facets. At higher ballistic frequency,  $\Gamma_b = 5.0 \text{ s}^{-1}$  in Fig. 3(c), the steady-state shape of the precipitate has evolved into a cuboidal shape with  $\{100\}$  facets and with rounded summits and edges. Upon further increase of  $\Gamma_b$ , the precipitate retains this shape up to a critical value

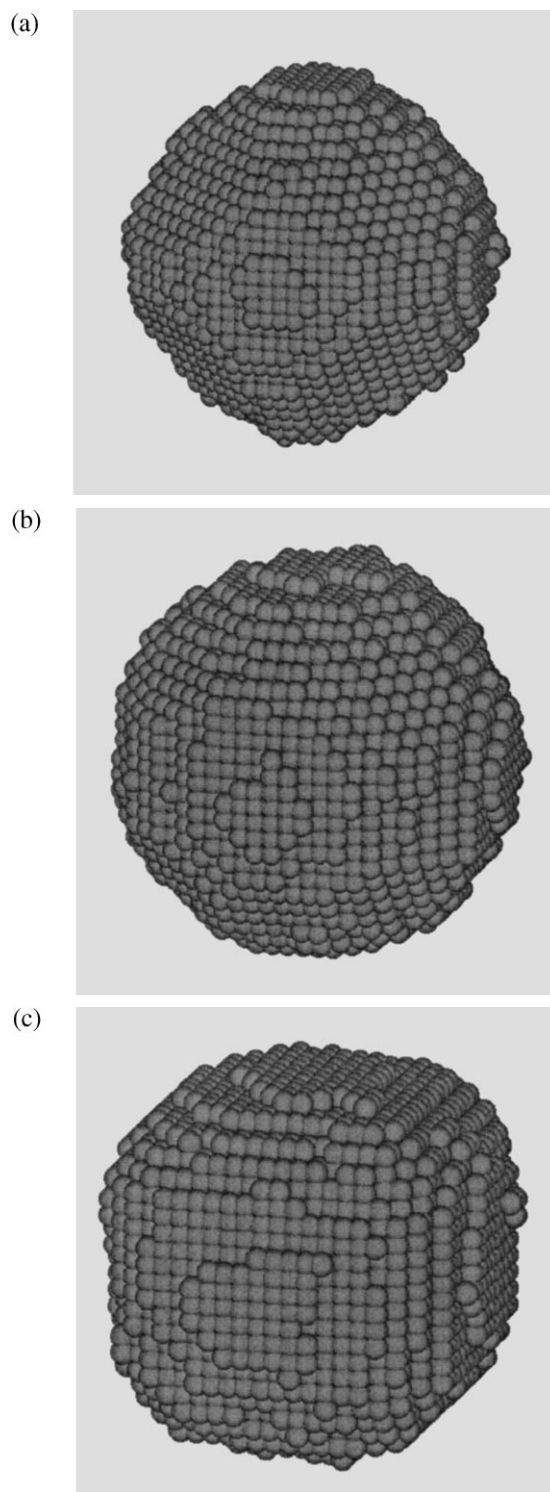


FIG. 3. Typical steady-state precipitate shapes at  $T = 400$  K as observed near  $[100]$  for (a)  $\Gamma_b = 0 \text{ s}^{-1}$ , (b)  $\Gamma_b = 0.5 \text{ s}^{-1}$ , and (c)  $\Gamma_b = 5 \text{ s}^{-1}$ . The simulation cell is  $64^3$ ; dark spheres represent sites of the cubic coarse-grained lattice lying at the precipitate-matrix interface.

$\Gamma_b = 14.5 \text{ s}^{-1}$  where the precipitate is dissolved. This nonequilibrium faceted shape is in agreement with the kinetic faceting observed for  $\{100\}$  bilayers.

From the current knowledge of phase stability in dynamical systems, the reported precipitate shape evolution is puzzling. The effective temperature criterion derived by Martin [11] for driven alloys would predict that interfaces become rough when the effective temperature  $T_{\text{eff}} = T \times (1 + \gamma) > T_R$ , where  $T_R$  is the equilibrium roughening transition temperature,  $\gamma = \Gamma_b / \langle \Gamma_{\text{th}} \rangle$  is a reduced ballistic jump frequency, and  $\langle \Gamma_{\text{th}} \rangle$  is an average frequency for thermally activated jumps. The nature of the kinetic roughening observed in our simulations is, however, very different from the equilibrium roughening transition, which is of the Kosterlitz-Thouless type. Furthermore kinetic faceting cannot be rationalized by this simple effective temperature rule. A clue may be found in approaches where one assumes the existence of an effective Hamiltonian that would describe the probabilities of microscopic steady states [4,7,18]. It has been shown that even with short-range pairwise physical interactions, effective interactions entering the effective Hamiltonian may become long ranged, and may include many-body interactions [18]. Further work is required to calculate the strength and range of these effective interactions as a function of the control parameters.

The atomic diffusion model used in this study relies on several approximations. Point defects are treated as conservative species, and interstitials are ignored. Atom interactions are treated as pairwise energies and stress effects are ignored. Furthermore, while isolated ballistic exchanges between nearest neighbors are a good approximation of the forced mixing created by high energy electrons in solids, they do not reproduce the complex dynamics that takes place in energetic displacement cascades [19]. Despite these limitations, kinetic roughening and kinetic faceting should be observable in alloys under irradiation. Indeed, for both kinetic roughening and faceting the key contribution of the ballistic exchanges is the sustained injection across the interface of  $B$  (respectively,  $A$ ) atoms into the  $A$ -rich (respectively,  $B$ -rich) phase. Such events are observed in molecular dynamic simulations of 1 keV displacement cascades near interfaces [20], and more recently for 5 keV cascades at Cu/Co and Ni/Cu interfaces [21]. Furthermore, the fact that interfaces may become diffuse under irradiation is in agreement with many ion-beam mixing experiments [2,19]. Finally, the restriction imposed on ballistic exchanges to occur between nearest neighbors is not unrealistic for fcc crystals: More than two-third of atom relocations produced by 10 keV cascades in Cu and Ni takes place between first nearest-neighbor sites [19]. The jumps beyond the first neighbor shell will increase the diffuseness of the interface and should therefore favor kinetic faceting over kinetic roughening.

While there have been many experimental reports of kinetic roughening at surfaces, very few studies have been published on the kinetic roughening of interfaces between crystalline phases. The latter measurements are difficult because they require techniques that are able to separate the roughness from the diffuseness of an interface. Preliminary results on Cu/Nb interfaces irradiated at various temperatures with 2 MeV  $\text{Kr}^+$  ions indicate that interfaces are mostly diffuse (and may be amorphous) after an 80 K irradiation, while a small amount of roughness exists after a 583 K irradiation [22]. No experimental evidence of kinetic faceting is so far available. If kinetic faceting can be achieved by optimizing irradiation conditions, it will promote an excellent thickness control in the case of implantation of layered structures. Preliminary simulation results also indicate that the modification of precipitate shapes under irradiation will alter their growth rate, as well as impurity segregation at these precipitates.

This work was supported by the U.S. Department of Energy, Basic Energy Sciences, Grant No. DEFG02-96ER45439 through the University of Illinois Materials Research Laboratory. Computing time has been obtained thanks to an IBM Shared University Research grant, and thanks to the generosity of D. D. Johnson.

- 
- [1] G. Martin and P. Bellon, *Solid State Phys.* **50**, 189 (1996).
  - [2] L. C. Wei *et al.*, *J. Appl. Phys.* **81**, 613 (1997).
  - [3] T. Klassen *et al.*, *Acta Mater.* **45**, 2921 (1997).
  - [4] J. L. Lebowitz *et al.*, *Ann. Phys. (Paris)* **1**, 1 (1957).
  - [5] R. Kubo *et al.*, *J. Stat. Phys.* **9**, 51 (1973).
  - [6] S. Katz *et al.*, *J. Stat. Phys.* **34**, 497 (1984); **38**, 725 (1985).
  - [7] P. L. Garrido *et al.*, *Phys. Rev. Lett.* **62**, 1929 (1989).
  - [8] P. Meakin, *Phys. Rep.* **235**, 189 (1993).
  - [9] K.-t. Leung *et al.*, *Phys. Rev. Lett.* **61**, 1744 (1988).
  - [10] P. Bellon and R. S. Averback, *Phys. Rev. Lett.* **74**, 1819 (1995).
  - [11] G. Martin, *Phys. Rev. B* **30**, 1424 (1984).
  - [12] G. Forgacs *et al.*, in *Phase Transitions and Critical Phenomena*, edited by C. Domb and J. L. Lebowitz, (Academic, New York, 1991), Vol. 14, p. 135.
  - [13] C. Jayaprakash *et al.*, *Phys. Rev. B* **30**, 3916 (1984).
  - [14] J. Villain, *J. Phys. I (France)* **1**, 19 (1991).
  - [15] J. Amar and F. Family, *Phys. Rev. Lett.* **77**, 4584 (1996).
  - [16] J. Amar and F. Family, *Phys. Rev. B* **54**, 14071 (1996).
  - [17] M. D. Johnson *et al.*, *Phys. Rev. Lett.* **72**, 116 (1994).
  - [18] V. Vaks *et al.*, *Phys. Lett. A* **177**, 269 (1993).
  - [19] R. S. Averback *et al.*, *Solid State Phys.* **51**, 281 (1998).
  - [20] H. Gades *et al.*, *Phys. Rev. B* **51**, 14559 (1995).
  - [21] K. Nordlund and R. S. Averback, *Phys. Rev. B* (to be published).
  - [22] P. Partyka *et al.*, *MRS Symp. Proc.* **396**, 107 (1996).